

The hERG R56Q^{+/-} LQTS variant induces electrical instability in hiPSC-CMs that is rescued by the RPR260243 hERG activator

R. Venkateshappa¹, D.V. Hunter¹, P. Muralidharan¹, R.S. Nagalingam^{1,2}, G. Huen¹, S. Faizi¹, S. Luthra¹, E. Lin¹, Y.M. Cheng¹, J. Hughes¹, R. Khelifi¹, P. Dhunna¹, R. Johal¹, V. Sergeev¹, S. Shafaattalab¹, L.M. Julian³, D.T. Poburko¹, Z. Laksman⁴, G.F. Tibbits^{1,2,5}, T.W. Claydon¹

Running title: Rescue of hERG R56Q arrhythmogenicity by RPR260243

Supplementary Material

Material and Methods

hiPSC culture

All experiments were performed using WiCell iPS(IMR90)-1 cells, kindly gifted by Dr. G.F. Tibbits, and maintained on Matrigel® (Corning, CLS356234) coated 6-well cell culture plates in mTeSR™Plus (STEMCELL Technologies, 100-0276) following the manufacturer's standard culturing procedures. Cells were passaged when they reached 80% confluency, approximately every 4 days: hiPSCs were dissociated to small aggregates using Versene (Gibco, 15040066) and light mechanical disruption and seeded at a split ratio of 1:20 in mTeSR™ Plus.

Generation of gene-edited cell lines

To perform CRISPR-Cas9 editing of hiPSCs, we used an approach described previously in Ran *et al.* 2013¹. The pCCC vector, a variant of the pSpCas9(BB)-2A-GFP vector with the Cbh promoter exchanged for the full-length CAGGS promoter to increase efficiency in hiPSC², was kindly gifted by Dr. F. Lynn and used to express the R56Q sgRNA, Cas9, and GFP in hiPSC cells. The R56Q sgRNA design was performed using the CRISPR design tool from the Broad Institute at MIT (<http://crispr.mit.edu/>) and the guide with the closest PAM site to the hERG R56 target site was selected, synthesized, and inserted into the BbsI site of the pCCC vector as described in Ran *et al.* 2013. A 127 bp ssODN (synthesized by IDT as a 4 nmole Ultramer) complementary to the sense strand, with 38 bases (PAM-distal) and 89 bases (PAM-proximal) on either of the expected double stranded break site, was used to provide the template for homology directed repair and included the hERG c.167G>A (p.Arg56Gln mutation, as well as a silent mutation (c.174G>A) in the PAM site.

The day before transfection, hiPSCs were passaged into small clumps using Versene (Gibco, 15040066) and seeded at a density of 100,000-200,000 cells per well of a 24-well plate. The following day, 500 ng of pCCC-sgRNA vector and 10 pmol of the ssODN were transfected

25 into each well using Lipofectamine 3000 according to the manufacturer's guidelines. Media
26 changes with fresh mTeSR Plus™ were performed 12 and 24 h after the transfection reagents were
27 applied. Two days after transfection hiPSCs were dissociated into single cells using Accutase
28 (STEMCELL Technologies, 07920) and FACS was used (BD FACSAria Fusion Cell Sorter) to
29 select GFP-positive cells. Between 500-1,000 GFP-positive cells were plated into each well of a
30 6-well culture dish, which was coated with Matrigel® (Corning, CLS356234) and contained
31 mTeSR™ Plus supplemented with penicillin-streptomycin (Life Technologies, 15140122) and
32 CloneR™ (STEMCELL Technologies, 05888), to aid in the survival and growth of the
33 individually seeded cells. After 48-72 h the media was changed, and every-other-day media
34 changes were performed for the following 7-10 days until individual colonies could be isolated.
35 Individual colonies were identified under a microscope and manually transferred into a 96-well
36 plate for further growth and analysis.

37 A sample of cells from each clone were lysed using DirectPCR Lysis Reagent with
38 Proteinase K Solution (Viagen, 301-C and 501-PK) and the lysate was used as the PCR template
39 to amplify the region around the hERG R56 site. The PCR product was sent for Sanger sequencing
40 (GENEWIZ, Azenta Life Sciences) to determine the genotype of the clones. Clones that were
41 selected for further experiments were expanded and cryopreserved using mFreSR™ (STEMCELL
42 Technologies, 05855). Off-target sites were predicted using CRISPOR (<http://crispor.tefor.net/>)³;
43 the top three exonic off-targets sites in the ZNRF3, SUPT5H and SLC38 genes amplified by PCR
44 and Sanger sequenced. No off-target mutations were identified in the clones.

45 ***Directed differentiation of hiPSCs to cardiomyocytes***

46 Differentiation of the hiPSC clones was performed following the STEMdiff™ Ventricular
47 Cardiomyocyte Differentiation Kit protocol (STEMCELL Technologies, 05010). Briefly the

48 hiPSC clones were seeded as small aggregates onto Matrigel®-coated 12-well plates with
49 mTeSR™Plus and ROCK inhibitor 10 μM Y-27632 (Biogems, 1293823) at a density of 300,000-
50 500,000 cells/well 48 h prior to the start of differentiation. Upon reaching 95% confluency, a series
51 of timed media changes were performed according to the differentiation kit protocol and beating
52 monolayers could be identified approximately 7-10 days after the start of differentiation.

53 Beating hiPSC-CMs monolayers were dissociated following procedures in the
54 STEMdiff™ Cardiomyocyte Dissociation Kit (STEMCELL Technologies, 05025). Briefly, the
55 beating monolayer was washed with Dulbecco's Phosphate Buffered Saline (D-PBS, VWRL0119-
56 0500) and treated with STEMdiff™ Cardiomyocyte Dissociation Medium for 7–10 min at 37°C
57 and 5% CO₂. The dissociated cells were resuspended in STEMdiff™ Cardiomyocyte Support
58 Medium at low enough density onto a 12 mm glass coverslip (VWR, 89015-725) coated with 10
59 μg/ml fibronectin (Gibco, PHE0023) to yield single, beating hiPSC-CMs. The media was changed
60 to STEMdiff™ Cardiomyocyte Maintenance Medium after 24 h and was refreshed every 2 days.
61 Electrophysiological and immunocytochemical analysis of the cells was performed 4-10 days after
62 replating.

63 ***Cellular phenotyping of hiPSC-CM clones***

64 hiPSC-CMs were fixed with 4% paraformaldehyde in D-PBS (Thermo Scientific, 28906),
65 followed by a 0.1 % Triton X-100 (Thermo Scientific, 28314) in D-PBS solution permeabilization
66 for 15 min each at room temperature. Coverslips were then blocked with 4% normal goat serum
67 (MiliporeSigma, NS02L) in PBS for 1 h, PBS washed, and probed overnight at 4 °C with mouse
68 monoclonal anti-cTnT (1:1000) (Invitrogen, MA5-12960) and rabbit monoclonal anti-α-actinin
69 (Invitrogen, 710947). The following day the coverslips were incubated at room temperature for 2
70 h with secondary antibodies, Alexa Fluor 488-conjugated goat anti-mouse (1:1000) (Invitrogen,

71 A-11029) and Alexa Fluor 555-conjugated goat anti-rabbit (1:1000) (Invitrogen, A32732), and the
72 nuclei were counterstained stained with Hoescht 33342 (Abcam, ab228551). The cells underwent
73 a post-staining fixation with 4% paraformaldehyde solution for 5 min prior to the final PBS washes
74 and mounting onto microscope slides with ProLong Glass Antifade Mountant (Thermo Scientific,
75 P36980). Images were acquired on a Nikon Ti-E inverted epifluorescence microscope equipped
76 with a Zyla 5.5 CMOS camera using a 20x Superfluor objective with a 1.5x multiplier.
77 Fluorophores were excited with a Sutter Lambda XL light source and SmartShutter. Images were
78 captured using Nikon Elements software (version 4.30, Nikon).

79 RNA from hiPSCs and hiPSC-CMs was isolated using the RNeasy Mini Kit (Qiagen,
80 74004) and cDNA was synthesized using the Qiagen QuantiTect Reverse Transcriptase Kit
81 (Qiagen, 205311), both according to the manufacturer's guidelines. Primers were designed to
82 target unique regions within pluripotency (NANOG, POU5F1, SOX2, C-MYC, KLF4) and
83 cardiomyocyte-related (ACTN1, MYL2, KCNH2) genes as well as two reference genes (GJA1,
84 GAPDH). Products were visualized on a 2% agarose gel to show qualitative levels of transcripts
85 in the undifferentiated hiPSCs and the differentiated hiPSC-CMs.

86 The effect of the hERG R56Q CRISPR-Cas9 edit on relative membrane expression of
87 hERG1a and hERG1b protein was assessed using western blot from whole cell lysates. Total
88 protein from hiPSC-CM monolayers was isolated using RIPA lysis buffer (25 mM Tris-HCl pH
89 7.6, 150 mM NaCl, 1% NP-40, 1% sodium deoxycholate, 0.1% SDS) (Thermo Fisher Scientific,
90 89900) containing protease and phosphatase inhibitor cocktail (Sigma-Aldrich, PPC1010). The
91 protein suspension was centrifuged at 14,000 rpm for 20 min at 4°C to remove the cell debris. A
92 Bradford assay was used for the measurement of protein concentrations. For western blot analysis,
93 60 mg of total protein was loaded in each lane of 8 % SDS-polyacrylamide gels under reducing

94 conditions along with PageRuler Plus Prestained Protein Ladder (Thermo Fisher Scientific, 26620)
95 and transferred into 0.45 mm Immobilon-P membrane PVDF (Millipore, IPVH85R). Blots were
96 blocked with 5 % BSA or 5 % milk in TBST for 1 h at room temperature. For primary antibody
97 detection, blots were probed with 1 % BSA or 1 % milk in TBST at 4 °C overnight, followed by
98 washing three times with TBST for 10 mins and incubating with secondary antibody in TBST with
99 1 % non-fat milk for 1 h at room temperature. hERG transcripts and GAPDH loading control were
100 detected by SuperSignal West Atto Ultimate Sensitivity chemiluminescent substrate (Thermo
101 Fisher Scientific, A38554). Detected bands were quantified using ImageJ (NIH, USA) to measure
102 relative band intensity. Antibodies used were: hERG1a rabbit monoclonal (Cell Signaling, D1Y2J,
103 1:1,000); hERG1b rabbit polyclonal (Enzolifesciences, ALX-215-051, 1:1,000); GAPDH mouse
104 monoclonal (Proteintech, 60004-1-Ig, 1:20,000); Goat anti-Rabbit IgG HRP (Invitrogen, G-21234,
105 1:5,000); Goat anti-mouse IgG HRP (Invitrogen, G-21040, 1:5,000).

106 *Electrophysiology*

107 Electrophysiological recordings were performed using an Axon instruments 200B
108 amplifier and Digidata 1440 interface. Signals were acquired at 10 kHz sampling frequency and
109 low-pass filtered at 2 kHz from single beating cardiomyocytes using perforated patch clamp. A P-
110 97 puller (Sutter Instruments) was used to fashion borosilicate glass capillaries with a tip resistance
111 of 2.5-3 M Ω when filled with an internal solution containing (in mM): CaCl₂ 2, EGTA 5, HEPES
112 10, KCl 150, KOH, MgATP 5, NaCl 5, and supplemented with 140-170 μ g/ml amphotericin B
113 (pH 7.2 with KOH). Cells were continuously perfused at a rate of 2 ml/min with external solution
114 containing (in mM): CaCl₂ 1.8, Glucose 15, HEPES 15, KCl 5.4, MgCl₂ 1, NaCl 150, Na-Pyruvate
115 1 (pH 7.4 using NaOH). All compounds were dissolved in DMSO, and working stocks were
116 prepared in external solution containing <1% DMSO. All experiments were carried out at 37°C,

117 with the bath temperature monitored and maintained using a TC-344B Warner Instruments
118 temperature controller equipped with a bath chamber thermistor, a heated platform, and an in-line
119 perfusion heater.

120 To record I_{Kr} , cells were patched and monitored in current clamp mode for stable
121 ventricular action potentials (diastolic potential <-60 mV) before 5 min superfusion with external
122 solution containing 10 μ M nifedipine to stop beating. I_{Kr} was then recorded during 2 s voltage
123 clamp steps from -60 mV to +40 mV in 20 mV increments (holding potential was -40 mV)
124 followed by a 3 s step to -40 mV to monitor deactivation. I_{Kr} was measured again following 5 min
125 superfusion with 10 μ M dofetilide and the dofetilide-sensitive I_{Kr} current was used for analysis.

126 The time course of dofetilide-sensitive deactivating I_{Kr} tail currents at -40 mV was fitted
127 with a double exponential equation:

$$128 \quad I = A_{fast} \exp(t/\tau_{fast}) + A_{slow} \exp(t/\tau_{slow}) + C$$

129 where A_{fast} and A_{slow} are the current amplitudes of the fast and slow components, τ_{fast} and τ_{slow} are
130 the time constants of the fast and slow components, and C is the residual amplitude. To simplify
131 comparison of deactivation kinetics^{4,5}, the weighted average tau was calculated as:

$$132 \quad \tau_{weighted} = (A_{fast} \times \tau_{fast} + A_{slow} \times \tau_{slow}) / (A_{fast} + A_{slow})$$

133 To record action potentials, the threshold current injection was determined in each cell by
134 stimulating cells with increasing current amplitude until a constant 1:1 response was observed.
135 Following this, 1.5-2x this threshold current was employed during a range of programmed
136 stimulation regimens designed using the Axon 200B clampex software. We utilized a 4 ms
137 blanking pulse to eliminate artefacts associated with the 2 ms stimulation pulses. To record action
138 potentials during standard S1-S2 paired stimulations, a train of eight S1 stimuli was applied with
139 a constant cycle length before an S2 stimulus that was applied at varying coupling intervals from

140 500 to 110 ms. The dynamic stimulation procedure involved stimulating cells for 30 beats at
141 progressively shorter basic cycle lengths (BCLs) from 500 ms to 167 ms.

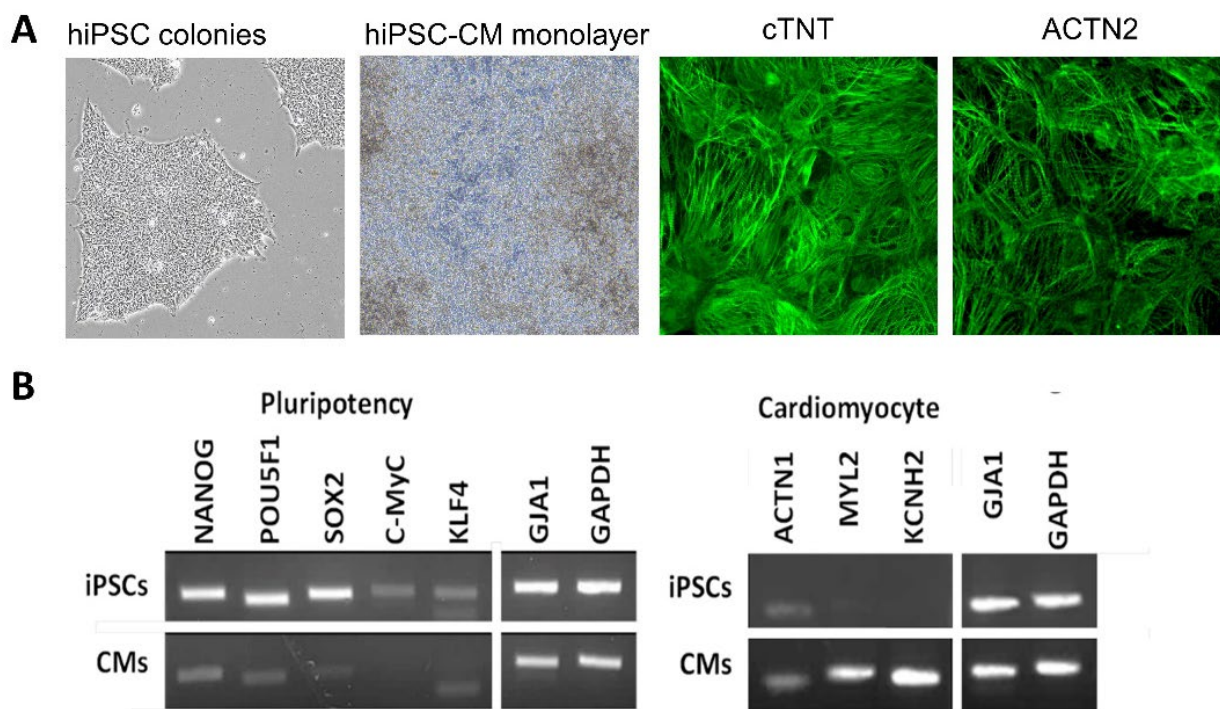
142

143

Results

144 **Figure S1. Cellular markers of hiPSC-CM differentiation**

145 hiPSC clones maintained characteristic features of hiPSCs and were successfully
146 differentiated into beating hiPSC-CMs monolayers that stained for cardiac troponin T (cTnT) and
147 alpha-actinin (ACTN2) in both a monolayer and when plated as individual cells (Figure S1A).
148 Although immature in nature, these hiPSC-CMs presented clear striation patterning of these
149 cardiac sarcomeric markers. This is further highlighted by RT-PCR measures demonstrating that
150 cardiomyocyte differentiation of the clones resulted in decreased expression of pluripotency
151 transcripts and increased expression of cardiomyocyte transcripts (Figure S1B).



152

153

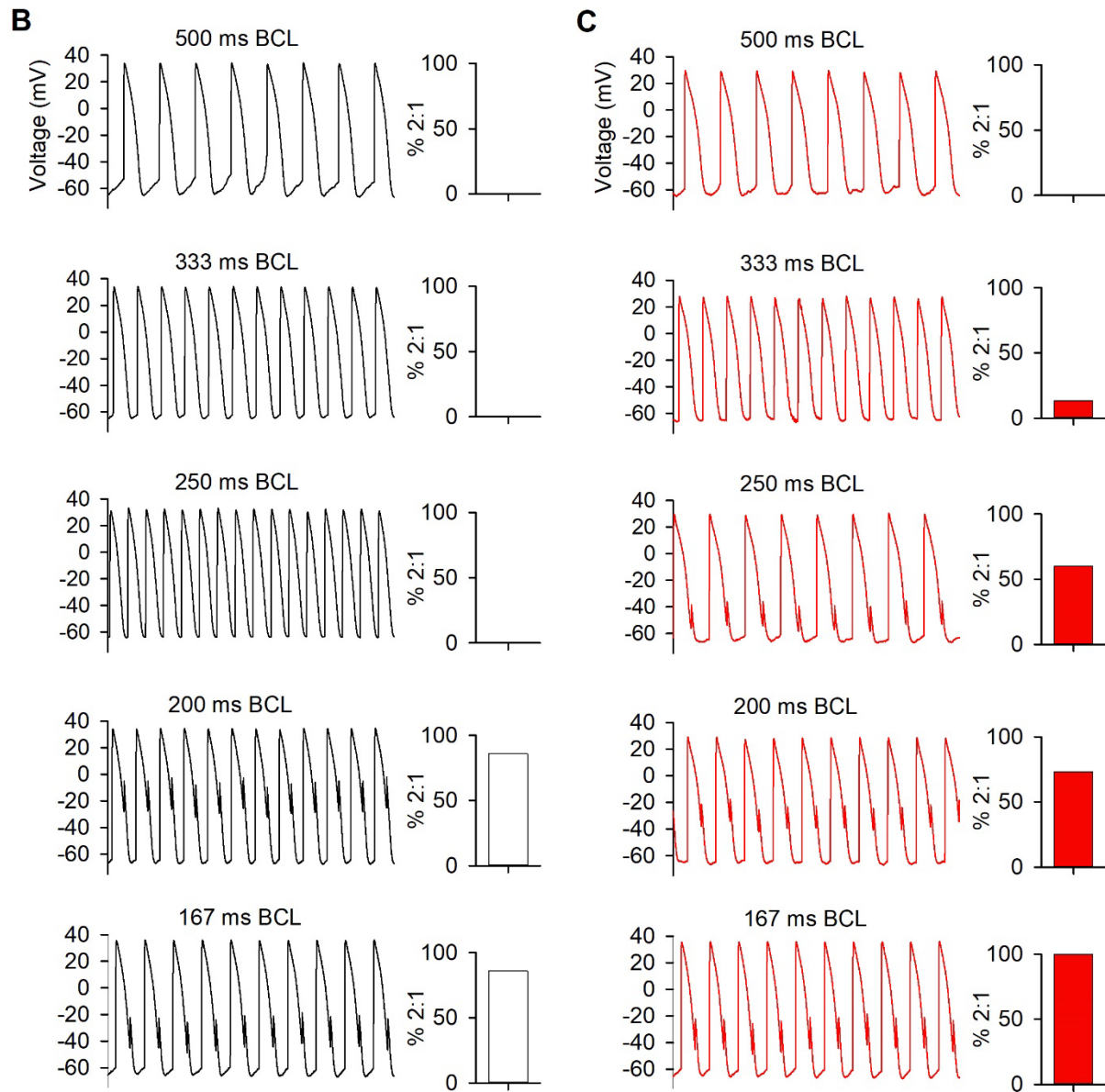
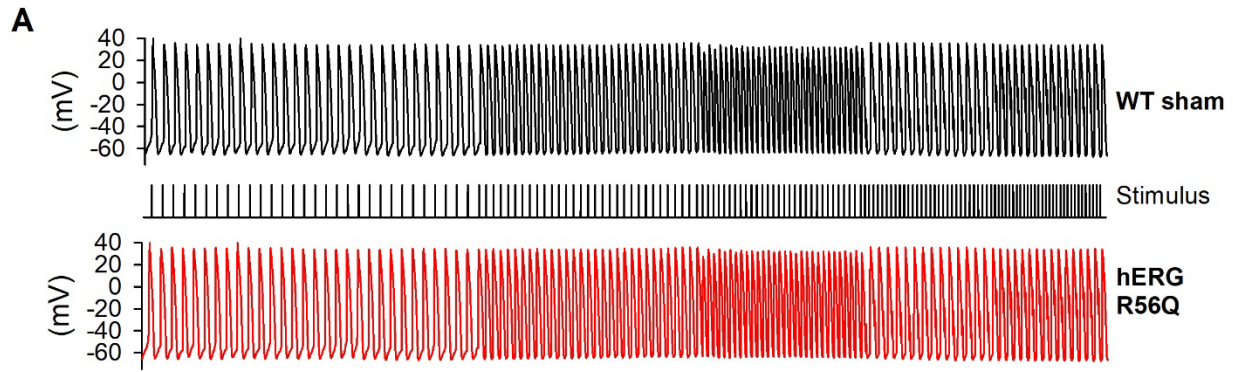
FIGURE S1

154

155 **Figure S2. Action potential restitution properties of hiPSC-CMs during dynamic rate**
156 **changes.**

157 Figure S2 shows representative membrane potential recordings in response to a stimulus
158 protocol designed to interrogate how action potentials adapt to dynamic changes in stimulus rate.
159 Example membrane responses obtained from a WT sham cell and a hERG R56Q cell are shown.
160 Figure S2A highlights the progressive action potential changes observed during 30 stimulations
161 applied at progressively shorter cycle lengths from a BCL of 500 ms to 167 ms. Action potentials
162 recorded during the final 5 s at each cycle length are shown on a slower time-base in Figure S2B-
163 C. Cells demonstrated 1:1 capture of action potentials with stimulations applied at longer BCLs
164 and progression to 2:1 capture at shorter BCLs. The percentage of cells displaying 2:1 capture at
165 each BCL is shown as bar charts. We observed an increased incidence in the loss of 1:1 capture at
166 shorter BCLs in hERG R56Q cells compared with WT sham cells. For example, at a BCL of 250
167 ms 1:1 capture was preserved in 100 % of WT sham cells, but only 40 % of hERG R56Q cells,
168 with 60 % of the latter group demonstrating 2:1 capture at this BCL.

169 The relationship between APD_{90} and DI during rate changes was used to plot dynamic
170 electrical restitution curves. The slope of the dynamic restitution curve was determined by fitting
171 the APD_{90} -DI relationship with a sigmoidal function and the average maximum slopes are shown.
172 We observed no remarkable differences across the conditions tested: maximum slope values were
173 2.0 ± 0.3 in WT sham (n=7), 1.7 ± 0.2 in WT sham with 10 μ M RPR260243 (n=7), 2.1 ± 1.1 in
174 hERG R56Q (n=15), and 2.3 ± 0.4 in hERG R56Q with 10 μ M RPR260243 (n=15).



175

176 **FIGURE S2**

177 **Table S1. Kinetics components of I_{Kr} deactivation in WT sham and hERG R56Q hiPSC-**
 178 **CMs.**

179 Deactivation gating of hERG channels is often described as a weighted average of the time
 180 constants yielded from bi-exponential fits to current decay. However, additional information may
 181 be gleaned from description of the two phases of deactivation kinetics. Table S1 summarizes the
 182 time constants and relative amplitudes of fast and slow phases of deactivation recorded from WT
 183 sham and hERG R56Q hiPSC-CMs in the absence and presence of RPR260243. The hERG R56Q
 184 variant accelerated the time constant of the slow phase of deactivation (p=0.022) and tended to
 185 reduce its relative contribution, although the latter did not reach statistical significance.
 186 Application of RPR260243 increased the relative contribution of the slow component of
 187 deactivation (p=0.034) and slowed the time constant of the fast component (p=0.012).

	A _{fast}	τ _{fast} (ms)	A _{slow}	τ _{slow} (s)
WT sham	0.57 ± 0.08	267 ± 50	0.43 ± 0.08	3.13 ± 0.54
hERG R56Q ^{+/-}	0.80 ± 0.07	158 ± 26	0.20 ± 0.07	1.02 ± 0.12*
hERG R56Q ^{+/-} + RPR260243	0.42 ± 0.11*	575 ± 151*	0.58 ± 0.11*	1.96 ± 0.52

188 *p<0.05

189 **TABLE S1**

190

191
192
193
194
195
196
197
198
199
200
201
202
203
204
205
206

References

1. Ran, F. A. *et al.* Genome engineering using the CRISPR-Cas9 system. *Nat Protoc* **8**, 2281–2308 (2013).
2. Krentz, N. A. J., Nian, C. & Lynn, F. C. TALEN/CRISPR-Mediated eGFP Knock-In Add-On at the OCT4 Locus Does Not Impact Differentiation of Human Embryonic Stem Cells towards Endoderm. *PLOS ONE* **9**, e114275 (2014).
3. Concordet, J.-P., Haeussler, M. & Haeussler. CRISPOR: intuitive guide selection for CRISPR/Cas9 genome editing experiments and screens. *Nucleic Acids Res* **46**, W242–W245 (2018).
4. Shi, Y. P., Thouta, S., Cheng, Y. M. & Claydon, T. W. Extracellular protons accelerate hERG channel deactivation by destabilizing voltage sensor relaxation. *J Gen Physiol* **151**, 231–246 (2019).
5. Ng, C.-A. *et al.* Heterozygous KCNH2 variant phenotyping using Flp-In HEK293 and high-throughput automated patch clamp electrophysiology. *Biology Methods and Protocols* **6**, bpab003 (2021).